



Cite this: *Dalton Trans.*, 2014, **43**, 17721

Photophysics and non-linear absorption of Au(I) and Pt(II) acetylide complexes of a thienyl-carbazole chromophore†

Subhadip Goswami,^a Geoffrey Wicks,^b Aleksander Rebane^{*b,c} and Kirk S. Schanze^{*a}

In order to understand the photophysics and non-linear optical properties of carbazole containing π -conjugated oligomers of the type ET-Cbz-TE (E = ethynylene, T = 2,5-thienylene, Cbz = 3,6-carbazole), a detailed investigation was carried out on a series of oligomers that feature Au(I) or Pt(II) acetylide "end groups", as well as a Pt(II)-acetylide linked polymer (**CBZ-Au-1** and **CBZ-Pt-1**, **CBZ-Poly-Pt**). These organometallic chromophores were characterized by UV-visible absorption and variable temperature photoluminescence spectroscopy, nanosecond transient absorption spectroscopy, open aperture nanosecond z-scan and two photon absorption (2PA) spectroscopy. The Au(I) and Pt(II) oligomers and polymer exhibit weak fluorescence in fluid solution at room temperature. Efficient phosphorescence is observed from the Pt(II) systems below 150 K in a solvent glass; however, the Au(I) oligomer exhibits only weak phosphorescence at 77 K. Taken together, the emission results indicate that the intersystem crossing efficiency for the Pt(II) chromophores is greater than for the Au(I) oligomer. Nonetheless, nanosecond transient absorption indicates that direct excitation affords moderately long-lived triplet states for all of the chromophores. Open aperture z-scan measurement shows effective optical attenuation can be achieved by using these materials. The 2PA cross section in the degenerate $S_0 \rightarrow S_1$ transition region was in the range 10–100 GM, and increased monotonically toward shorter wavelengths, reaching 800–1000 GM at 550 nm.

Received 12th July 2014,
Accepted 31st August 2014

DOI: 10.1039/c4dt02123a

www.rsc.org/dalton

Introduction

Since the discovery of two-photon absorption (2PA) by Göppert-Mayer in the 1930s¹ and the first experimental observation of the effect in 1961,² there has been significant research in this field, with investigations seeking to understand the factors that control the 2PA cross-section (σ_2) and to harness the effect in diverse applications. Two-photon absorption has a number of applications ranging from ultrafast optical power limiting *via* non-linear absorption (NLA),^{3–6} photodynamic therapy,⁷ microscopy,⁸ and three-dimensional data storage.^{9–11} Although a variety of organic dyes have proven to be efficient 2PA chromophores, heavy-metal containing organometallic chromophores are especially interesting, in

particular with respect to applications in frequency and temporal agile non-linear absorption.¹² Among various organometallic complexes, platinum acetylide containing π -conjugated chromophores are attractive for NLA materials because of their "dual mode" non-linear absorption mechanism.^{13–18} This dual mode comprises of ultrafast 2PA to produce the singlet excited state followed by intersystem crossing (ISC) to a long-lifetime triplet state T_1 promoted by the heavy atom effect, which can further absorb photons due to a strongly allowed T_1-T_n absorption.^{18,19}

Porphyrin^{20–23} and phthalocyanine^{24–26} metal complexes have been widely investigated with respect to 2PA and long pulse NLA *via* the dual mode mechanism; however, metal complexes linked to π -conjugated segments that feature the carbazole moiety have not been well explored.²⁷ Even though the singlet excited state photophysics for carbazole containing oligomers and polymers are well established, the triplet excited state is relatively unexplored. Introduction of a heavy metal such as platinum or gold into the conjugated backbone of carbazole containing oligomers provides insight into the triplet excited state due to the "heavy atom effect" that is elusive in the strictly organic system.^{28–31} Most carbazole derivatives find application in OLEDs or bulk heterojunction solar cells as π

^aDepartment of Chemistry, University of Florida, P.O. Box 117200, Gainesville, FL 32611, USA. E-mail: kschanze@chem.ufl.edu; Tel: +1-352-392-9133

^bPhysics Department, Montana State University, Bozeman, Montana 59717, USA. E-mail: rebane@physics.montana.edu; Tel: +1-406-994-7831

^cNational Institute of Chemical Physics and Biophysics, Tallinn, EE 12618, Estonia
†Electronic supplementary information (ESI) available: Detailed description of the synthesis and characterization of **CBZ-Au-1**, **CBZ-Pt-1** and **CBZ-Poly-Pt**. Experimental set up for non-linear transmission (NLT) and transmission vs. incident laser pulse energy plot. See DOI: 10.1039/c4dt02123a

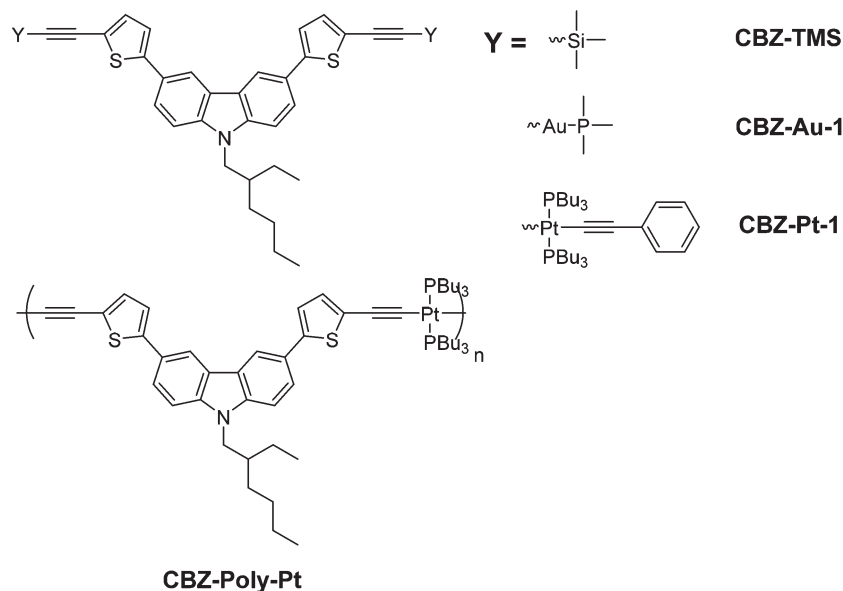


Chart 1

electron donor materials; however, there are few reports on organometallic carbazole complexes that exhibit non-linear absorption.²⁷ Zhou *et al.* reported a carbazole platinum acetylide polymer and a model platinum complex substituting 3,6 position of the aromatic ring, as an efficient optical power limiting material at 532 nm.³² Tao *et al.* reported a naphthalene platinum acetylide substituted carbazole as a two photon absorbing and two photon induced luminescence molecule with a 2PA cross section (σ_2) of 14 GM ($\lambda_{\text{ex}} = 740 \text{ nm}$).³³

In order to gain fundamental insight into the photophysics and non-linear optical properties of carbazole containing π -conjugated oligomers of the general structure ET-Cbz-TE (T = 2,5-thienylene, Cbz = 3,6-carbazole and E = ethynyl), here we report a detailed investigation of a series of complexes that feature Au(I) or Pt(II) acetylide “end groups”, as well as a Pt(II)-acetylide linked polymer (CBZ-Au-1 and CBZ-Pt-1, CBZ-Poly-Pt in Chart 1). We were particularly interested in developing NLA chromophores that have high transparency throughout the visible region, and as such the 3,6-substitution pattern on the Cbz was used which gives rise to a relatively large HOMO-LUMO gap³⁴ and consequently good optical transparency through most of the visible region. The photophysical properties of the series of complexes and polymer are fully analyzed, including one and two-photon absorption spectra, photoluminescence spectra, triplet-triplet absorption spectra and singlet oxygen sensitization studies. The results clearly suggest that this set of chromophores has the potential to be used in optical power limiting materials, and the results shed light on how the yield of the triplet state depends on the nature of the heavy metal center. Previous studies have examined in some detail the photophysics of π -conjugated oligomers linked to heavy metals, and this work builds on that base of understanding.^{35–37}

Experimental section

Synthesis

The details of the synthetic procedures along with the synthetic scheme and all the characterizations are provided in the ESI.†

Instrumentation and methods

All the NMR spectra were recorded using a Varian VXR-300 FT-NMR, operating at 300 MHz for ^1H NMR, 121 MHz for ^{31}P NMR and at 75.4 MHz for ^{13}C NMR. Mass spectrometry for the newly synthesized compounds were recorded on a Bruker APEX II 4.7 T Fourier Transform Ion Cyclotron Resonance mass spectrometer (Bruker Daltonics, Billerica, MA). Gel permeation chromatography (GPC) analysis of the polymer was performed on a system containing a Shimadzu SPD-20A photodiode array (PDA) detector, using THF as eluent at 1 ml min^{-1} flow rate and the system was calibrated with respect to linear polystyrene standards in THF.

Photophysical measurements were conducted with dry HPLC grade THF as solvent in $1 \times 1 \text{ cm}$ quartz cuvettes unless otherwise noted. UV-visible absorption spectra were obtained on a Varian Cary 100 dual beam spectrophotometer. Room temperature and low temperature emission spectra were recorded on a Photon Technology International (PTI) fluorimeter and collected 90° relative to the excitation beam. The optical density of the sample solutions was kept at ≤ 0.1 at excitation wavelength. Refractive index corrections were applied for sample and standard solutions for emission quantum yield measurements. Freshly distilled HPLC grade 2-methyl tetrahydrofuran was used for the low temperature experiments. The sample was placed in 1 cm diameter borosilicate glass tube and deoxygenated by 4–5 freeze-pump-thaw cycles under

vacuum (10^{-5} Torr) prior to use. Temperatures to 77 K were achieved by using liquid-nitrogen-cooled Oxford instrument DN 1704 optical cryostat attached to an Omega CYC3200 auto-tuning temperature controller. The reported concentration for polymer refers to the concentration of polymer Repeat Unit (PRU). Solutions for spectroscopic studies were prepared by dilution of stock solutions. Fluorescence lifetimes were collected *via* a FluoTime 100 Fluorescence Lifetime Spectrometer (PicoQuant, USA).

Nanosecond timescale transient absorption spectroscopy was conducted on a home-built apparatus using the third harmonic of a Continuum Surelite series Nd:YAG laser ($\lambda = 355$ nm, 10 ns FWHM, 7 mJ per pulse). Probe light was produced by a xenon flash lamp and the transient absorption signal was detected with a gated-intensified CCD mounted on a 0.18 m spectrograph (Princeton PiMax/Acton Pro 180). Samples for transient absorption were contained in a 1 cm path length flow cell with a total volume of 10 ml and continuously circulated at the pump-probe region during the experiment. The optical density of the solutions was kept ≈ 0.7 at 355 nm and samples were degassed with argon for at least 45 minutes before the measurement. Singlet oxygen quantum yields were measured using a Photon Technology International Quantmaster near-IR spectrophotometer containing an InGaAs photodiode detector, an optical chopper and a lock-in amplifier. The optical density was kept below 0.12 for all the samples at excitation wavelength 350 nm.

The open aperture nanosecond time domain z-scan measurements were performed on a system which employs the third harmonic output of a Continuum Surelite II Nd:YAG laser equipped with a Continuum Surelite OPO PLUS for excitation at 600 and 628 nm. All of the chromophores were excited with a 600 nm laser beam through 50/50 beam splitter. The beam was focused using 50.8 mm focus length, 38.1 mm diameter plano-convex lens. Sample solutions ($C = 1.0$ mM) were taken in a 1 mm path length cuvette and moved along the focused beam using a manual one-directional translational stage placed exactly behind the focusing lens. The energy of the laser beams were obtained by using Ophir pyroelectric heads and an Ophir Laserstar power/energy monitor and collected using StarCom32 software.

The laser system for the 2PA measurements comprised a Ti:Sapphire femtosecond oscillator (Lighthouse Inc.), femtosecond regenerative amplifier (Legend F-HE, Coherent Inc.), and an optical parametric amplifier, OPA (TOPAS-C, Light Conversion). The second harmonic of the signal output of the OPA was continuously tunable from 540 to 810 nm with the maximum pulse energy in the range 10–30 μ J, and second harmonic of the idler was tunable from 800 to 1070 nm with the maximum pulse energy 10–30 μ J. The average pulse duration was 80–120 fs (FWHM). A detailed description of the laser system is provided elsewhere.³⁸ The NLT method has been described previously.^{18,39–41} (The schematic of the NLT apparatus is provided in Fig. S12†). Briefly, the OPA output beam at 100 Hz pulse repetition rate was directed through the sample prepared at concentration, $C \sim 10^{-3}$ M, in a standard 10 mm

spectroscopic cuvette. Two identical 10 mm diameter silicon photodetectors (Thorlabs, DET100A) were used to measure the laser pulse reflected from two glass beam pick-off plates positioned accordingly, before and after the sample. The analog signals from the photodetectors were digitized using a DAQ board (National Instruments, Model PCI-6110). The dependence of the sample transmission (defined as ratio of the signal from the second detector divided by the signal from the first detector) on the incident intensity was evaluated by varying the energy of the incident pulse in the range $P_{in} \approx 0.3$ –30 μ J using a neutral density filter attenuator wheel (Thorlabs) mounted on a stepper motor (Fig. S13 in the ESI† shows typical measured dependence of the transmission on the incident pulse energy at different wavelengths). The estimated accuracy of the measured transmission is about 0.1%. A laser power meter (Nova II, Ophir) was used to measure the average laser power at the input to the sample. The beam diameter at the sample was 0.8–1.5 mm and varied depending on the OPA. For calibration of the 2PA cross section a known reference PPV in THF was measured under identical conditions.¹⁸

Results and discussion

Ground state absorption spectra

The absorption spectra of the TMS-protected oligomer **CBZ-TMS**, metal complexes **CBZ-Au-1**, **CBZ-Pt-1** and polymer **CBZ-Poly-Pt** were measured in THF solution and are shown in Fig. 1a, and the molar extinction coefficients (ϵ) and absorption band maxima (λ_{max}) are listed in Table 1. In general, the metal complexes, polymer and the free oligomer show strongly allowed absorption in the 300–450 nm region. However, there are interesting and significant differences in the absorption properties across the series. First, the absorption of the free oligomer **CBZ-TMS** is the most blue shifted of the series, with the principal π, π^* transition lying in the near-UV with an onset ~ 410 nm and $\lambda_{max} = 328$ nm. Second, the absorption of the gold(i) congener, **CBZ-Au-1**, is quite similar to that of **CBZ-TMS**, but the onset and λ_{max} are slightly red-shifted. This fact can be attributed to the weak interaction between 5d orbitals of the Au(i) centers with the ligand π system.⁴² Interestingly, the absorption of the Pt(ii) complex and polymer are significantly red-shifted and show enhanced molar absorptivity compared to the free oligomer and Au(i) complex. The absorption onsets are red-shifted by ~ 25 nm, and the enhanced oscillator strength for the Pt(ii) systems is clearly due to enhanced π -conjugation due to mixing of the ligand π -levels with the $d\pi$ levels of the Pt(ii) centers,⁴³ (The enhanced molar absorptivity of **CBZ-Pt-1** compared to **CBZ-Poly-Pt** is in part artifact arising because the polymer repeat unit used in the calculation of the absorptivity contains only a single Pt(ii) acetylide unit, whereas oligomer **CBZ-Pt-1** contains two). Taken together, these results suggest that there is substantial metal–ligand electronic interaction in the Pt(ii) systems; however, the interaction is at best weak in the Au(i) complex.

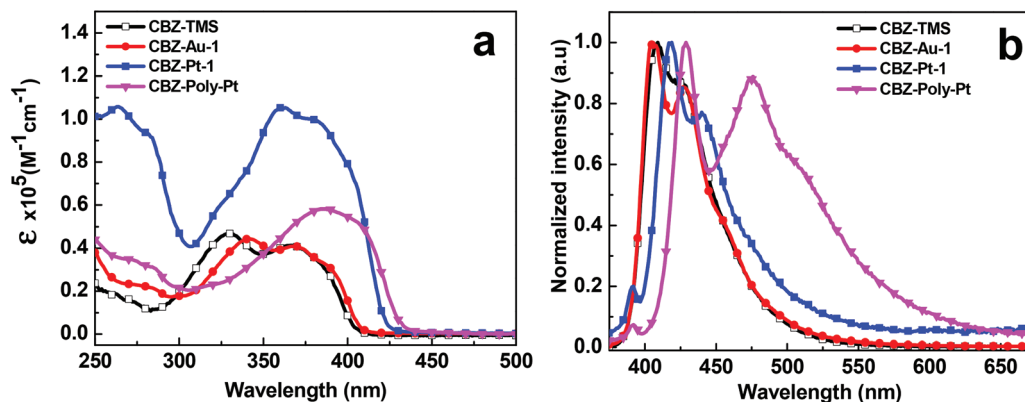


Fig. 1 (a) Absorption and (b) room temperature emission spectra of CBZ-TMS, CBZ-Au-1, CBZ-Pt-1 and CBZ-Poly-Pt in THF solution. The emission spectra were obtained with excitation wavelength at 350 nm and they are intensity normalized at λ_{\max} . Note that the molar absorptivity for CBZ-Poly-Pt is based on the repeat unit concentration, where the repeat unit contains a single Pt(II) center.

Table 1 Photophysical properties in THF solution

Compound	λ_{\max}/nm	$\epsilon/\text{M}^{-1} \text{cm}^{-1}$	$\lambda_{\text{F}}/\text{nm}$	Φ_{F}^a	$\lambda_{\text{Phos}}/\text{nm}^b$	$\tau_{\text{F}}/\text{ns}^c$	Φ_{Δ}^d	$\tau_{\text{TA}}/\mu\text{s}$
CBZ-TMS	328	46 000	407	0.43	—	—	—	0.36
CBZ-Au-1	341	44 000	406	0.04	591	<0.2	0.21 ± 0.02	0.63
CBZ-Pt-1	362	105 000	418	0.003	605	<0.2	0.15 ± 0.02	0.42
CBZ-Poly-Pt	386	58 000	428	0.01	610	<0.2	0.16 ± 0.02	0.34

^a Fluorescence quantum yield was measured with respect to quinine sulfate in 0.1 M sulfuric acid ($\Phi_{\text{F}} = 0.54$), and the estimated error is $\pm 5\%$.

^b Phosphorescence was measured in distilled 2-MeTHF solvent. ^c Lifetime was shorter than lower limit of the picoQuant instrument, 200 ps. All samples are excited at 375 nm. The emission was detected for CBZ-Au-1 at 400 nm and for CBZ-Pt-1 and CBZ-Poly-Pt at 425 nm. ^d Singlet oxygen quantum yield was determined in C_6D_6 using terthiophene ($\Phi_{\Delta} = 0.73$) as actinometer.

Steady-state photoluminescence spectroscopy

Room temperature photoluminescence spectra of the oligomer CBZ-TMS, metal complexes CBZ-Au-1, CBZ-Pt-1 and the polymer CBZ-Poly-Pt in deoxygenated THF are shown in Fig. 1b. At ambient temperature, and with excitation at $\lambda = 350$ nm, vibronically structured emission bands were observed that show comparatively low Stokes shift from the absorption. The lifetimes of this emission from the metal complexes (τ_{F} , Table 1) are very short (<200 ps), and on the basis of the small Stokes shift and short lifetimes the emission is attributed to fluorescence from the $^1\pi,\pi^*$ state.²⁸ The fluorescence spectra show similar trends across the series as noted for the UV-visible absorption spectra. In particular, the emission maxima are red-shifted from free oligomer CBZ-TMS in the sequence CBZ-Au-1 < CBZ-Pt-1 < CBZ-Poly-Pt. Two well defined vibronic peaks were observed in the fluorescence spectrum for all of the systems, which is a signature of 3,6-thienyl substituted carbazole system.⁴⁴ The fluorescence quantum yields (Φ_{F} , Table 1) for the metal complexes and polymer are more than an order of magnitude less than for the free oligomer CBZ-TMS, which can be attributed to efficient $\text{S}_1 \rightarrow \text{T}_1$ intersystem crossing in the former. Close inspection of the fluorescence quantum yield data suggests both the platinum complex CBZ-Pt-1 and the polymer CBZ-Poly-Pt exhibit the most efficient intersystem crossing to the triplet manifold, compared to gold(i) complex

CBZ-Au-1, which has a noticeably larger fluorescence yield. This fact can be attributed to stronger spin-orbit coupling effect for platinum(II) than gold(I).⁴³ Interestingly, gold(I) has a slightly larger spin-orbit coupling constant than platinum(II).⁴⁵ We believe that the larger spin-orbit coupling in the platinum(II) systems arises because there is greater $d\pi$ -metal/ π^* -ligand orbital mixing than in the gold(I) system.

In order to understand the effect of the different heavy atoms in promoting phosphorescence in the oligomers, variable temperature photoluminescence spectroscopy was performed on the series in deoxygenated 2-methyltetrahydrofuran (2-MeTHF) solvent (glass). As shown in Fig. 2, for the Pt(II) oligomer and polymer, below 130 K a structured emission band is clearly seen in the region from 590–800 nm that is assigned to phosphorescence from the T_1 state. Note that at 80 K, the emission is dominated by the phosphorescence, and given that the room temperature fluorescence yields are ~ 0.01 , we estimate that the 80 K phosphorescence yields for CBZ-Pt-1 and CBZ-Poly-Pt are in the range 0.05–0.10.

In contrast to the emission of the Pt(II) systems, even at 80 K the gold(I) complex CBZ-Au-1 exhibits vibronically structured fluorescence and only a weak phosphorescence emission (Fig. 3). The weak phosphorescence from CBZ-Au-1 can be attributed to less efficient spin-orbit coupling for gold(I) in comparison to platinum(II).⁴⁶ In all of the phosphorescence spectra, there are two distinct vibronic progressions observed,

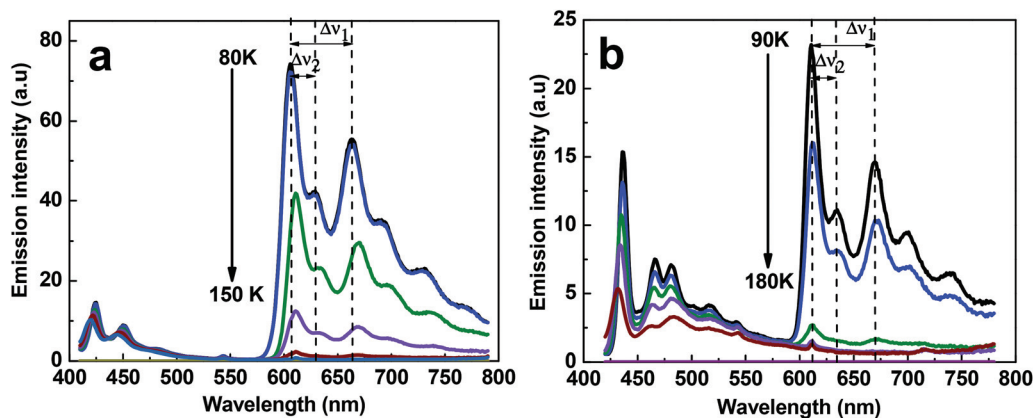


Fig. 2 Low temperature emission spectra of (a) platinum(II) oligomer CBZ-Pt-1 (temperatures are 80, 90, 100, 120, 135 and 150 K) and (b) platinum(II) polymer CBZ-Poly-Pt in 2-MeTHF (temperatures are 90, 110, 130, 150 and 180 K). The excitation wavelength was 350 nm. The frequencies of the vibronic progressions discussed in the text were determined by the differences shown in the figures.

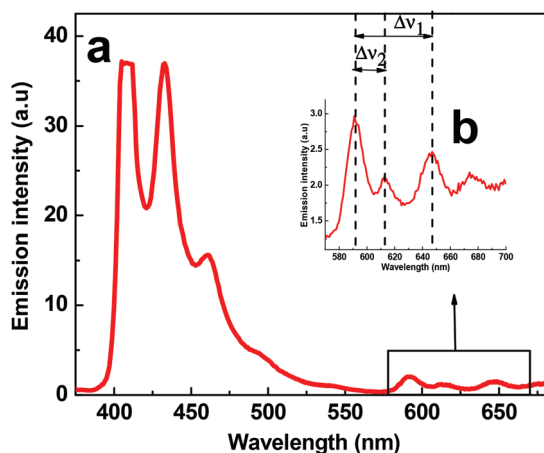


Fig. 3 Low temperature emission spectrum (77 K) of (a) gold(I) complex CBZ-Au-1 and (b) magnified phosphorescence region. Note that the 0–0 band in the fluorescence is clipped due to the scaling used to show the weak phosphorescence. The frequencies of the vibronic progressions discussed in the text were determined by the differences shown in b.

assigned as $\Delta\nu_1$ and $\Delta\nu_2$. The coupling frequency differs slightly from sample to sample. The $\Delta\nu_1$ is 1430 cm^{-1} for CBZ-Pt-1 and CBZ-Au-1, whereas for CBZ-Poly-Pt $\Delta\nu_1 \approx 1460\text{ cm}^{-1}$. For CBZ-Pt-1, CBZ-Au-1 and CBZ-Poly-Pt $\Delta\nu_2 \approx 610$, 575 and 660 cm^{-1} , respectively. The low temperature fluorescence spectra of CBZ-Pt-1 and CBZ-Au-1 exhibit a progression with nearly the same frequency ($\Delta\nu_1 \approx 1430\text{ cm}^{-1}$) as the high frequency progression in the phosphorescence. Interestingly, the fluorescence of the polymer exhibits two progressions, one at a similar frequency ($\Delta\nu_1 \approx 1430\text{ cm}^{-1}$) and another a higher frequency ($\Delta\nu_1 \approx 2090\text{ cm}^{-1}$). The latter may be due to coupling of the singlet state with the C≡C modes.

Transient absorption spectroscopy

To further explore the properties of the triplet state, ns– μ s transient absorption spectroscopy was carried out on deoxygenated

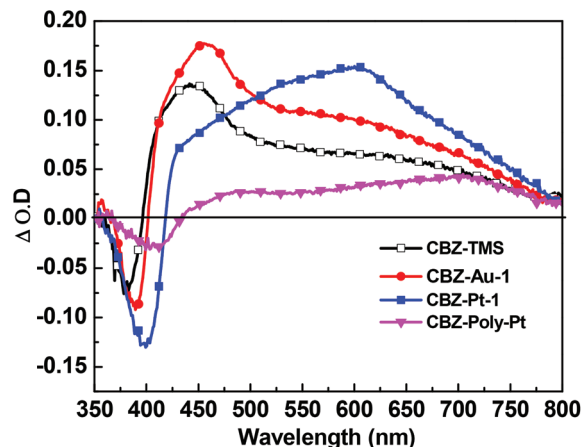


Fig. 4 Nanosecond transient absorption spectra of the ligand CBZ-TMS, metal complexes CBZ-Au-1, CBZ-Pt-1 and the polymer CBZ-Poly-Pt in deoxygenated THF solution for 45 minutes. All samples were excited at 355 nm with 300 ns of camera delay increment. All the samples have matched absorbance of ~ 0.7 at the excitation wavelength.

THF solutions of the oligomers and polymer. Fig. 4 compares the transient absorption spectra of oligomer CBZ-TMS with CBZ-Au-1, CBZ-Pt-1 and CBZ-Poly-Pt, immediately following the laser pulse in THF. The transients are quenched by oxygen, and on this basis they are assigned to the absorption of the lowest triplet excited state. The lifetimes of the transient absorption of the triplet state are listed in Table 1 (τ_{TA}). The triplet lifetimes for the oligomers are similar, ranging from 0.35 – $0.65\ \mu\text{s}$, and they vary in the sequence CBZ-Au-1 > CBZ-Pt-1 > CBZ-Poly-Pt. The difference absorption spectra generally consist of ground state bleaching of the S_0 – S_1 absorption and broad T_1 – T_n absorption in the visible region. Interestingly CBZ-TMS also exhibits triplet absorption, possibly due to the presence of the thiophene units, which are known to enhance ISC in π -conjugated electronic systems.⁴⁷

The λ_{max} for T_1 – T_n absorption is shifted about 20 nm for the gold complex CBZ-Au-1 and ~ 164 nm for the platinum

complex **CBZ-Pt-1** relative to the ligand **CBZ-TMS**. By comparing the transient absorption signal of the metallated oligomers with the polymer, it is found that the intensity of the signal for the polymer is lower. As the experiment is carried out from samples solutions of matched absorbance, with the same laser power, and the same excitation wavelength, this difference suggests either that the polymer **CBZ-Poly-Pt** has a lower triplet yield than the metal complexes, or that there is a triplet quenching pathway that operates in the polymer that is not available in the oligomers. One possibility is that triplet-triplet annihilation may take place in the polymer.

As direct excitation of the metal complexes and the polymer produces the triplet state, we examined their ability to sensitize the generation of singlet oxygen ($^1\text{O}_2$) in deuterated benzene solution. These experiments were performed by monitoring phosphorescence from $^1\text{O}_2$ at 1270 nm. All of the materials sensitize the production of singlet oxygen, with observed quantum yields ranging from 0.15–0.21 (Φ_Δ , Table 1), consistent with moderately efficient intersystem crossing. However, the singlet oxygen yields are somewhat less than might be expected given that the fluorescence quantum yields of the metallated oligomers are so much less than free oligomer. This may be due to the relatively short triplet lifetimes which result in incomplete triplet energy transfer to oxygen whose concentration is comparatively low in the air saturated solutions.

Two photon absorption spectroscopy

Two photon absorption spectra and cross sections of **CBZ-Au-1**, **CBZ-Pt-1** and **CBZ-Poly-Pt** were measured in THF by the non-linear transmission (NLT) method and are presented in Fig. 5. The comparatively low fluorescence quantum yields for the metal containing oligomers and polymer precluded the use of the two photon excited fluorescence (2PEF) method. The normalized ground state absorption spectra are shown in the plots for comparison. In all three compounds the 2PA cross section values are relatively low in the $S_0 \rightarrow S_1$ transition region, $\sigma_{2PA} \sim 10\text{--}100$ GM, with only **CBZ-Au-1** showing slightly higher values. The cross section intensity increases rapidly toward shorter wavelengths, reaching values of $\sigma_2 \sim 800\text{--}1000$ GM at 550 nm. Because the maxima of the 2PA spectra are blue-shifted relative to the ground state absorption maxima, we may conclude that these systems display mainly centrosymmetric character.⁴⁸ Comparison of the nanosecond transient absorption and 2PA spectra shows that there is a significant overlap between them, especially in the mid-visible region between 500 and 650 nm. This overlap suggests that the complexes will exhibit pronounced long-timescale non-linear absorption *via* the dual mode mechanism that combines 2PA and excited state absorption by the triplet state.

In order to probe the ability of the oligomers and polymers to display non-linear absorption *via* the dual mode mechanism, open-aperture z-scan experiments were performed by using 1 mM THF sample solutions with 600 nm, 5 ns pulses. Note that 600 nm is more than 100 nm to the red of the onset of the allowed singlet ground state absorption transition, and

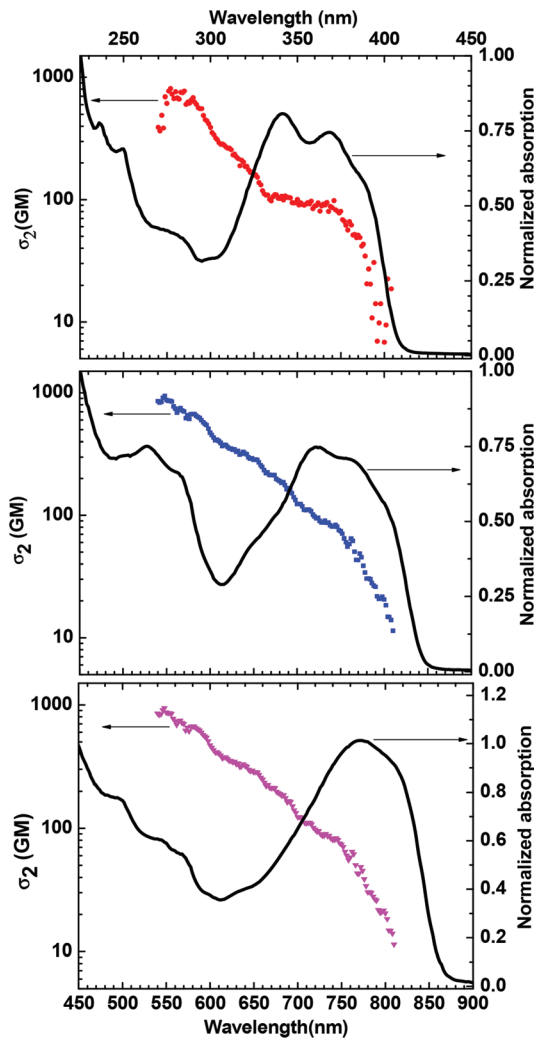


Fig. 5 2-Photon absorption spectra of the metal complexes and the polymer are measured with femtosecond pulses *via* the non-linear transmittance method in THF solution (red filled circles for **CBZ-Au-1**, blue filled squares for **CBZ-Pt-1** and magenta filled diamonds for **CBZ-Poly-Pt**); corresponding wavelengths are in bottom horizontal scale. One photon absorption spectra (shown by black line) are measured in THF solution and corresponding wavelengths are in upper horizontal scale.

consequently excitation at this wavelength is only likely to occur *via* 2PA. Fig. 6 compares the representative z-scan results for **CBZ-Au-1**, **CBZ-Pt-1** and **CBZ-Poly-Pt**. From the z-scan result, it is evident that the non-linear response of these materials varied in the series **CBZ-Poly-Pt** \sim **CBZ-Pt-1** $>$ **CBZ-Au-1**, with the Pt-oligomer and polymer sample exhibiting approximately 10% reduction in transmittance at the peak of the z-scan. Recent work from our laboratories has explored the nanosecond z-scan response of a series of Pt-acetylide complexes with high 2PA cross section conjugated ligands.⁴⁹ The z-scan response for the present series of carbazole oligomers are somewhat less compared to that of the most active Pt-acetylide oligomers previously investigated. The attenuated response is likely due to the fact that the σ_2 values for the carbazole based

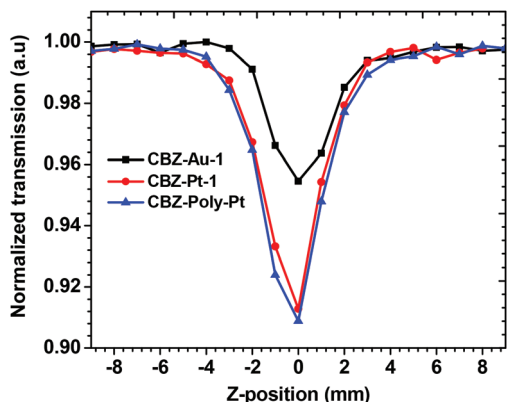


Fig. 6 Open aperture nanosecond z-scan 1 mM THF solution of CBZ-Au-1, CBZ-Pt-1 and CBZ-Poly-Pt at 600 nm excitation wavelength, 5 ns pulse width.

oligomers are lower compared to the previously investigated systems. Nonetheless, the response observed in the present series of complexes is respectable and given their relatively good optical transparency, especially for CBZ-Au-1, these chromophores may be useful in non-linear optical applications.

Summary and conclusions

This study highlights the photophysical and non-linear absorption properties of a novel series of organometallic chromophores that are based on the carbazole containing ET-Cbz-TE π -conjugated oligomer. The results provide insight regarding the relative effects of the Au(I) and Pt(II) centers on S_1 - T_1 intersystem crossing, radiative decay of T_1 (phosphorescence), and non-linear absorption. Au(I) appears to have relatively little effect on the ground state absorption of the ET-Cbz-TE chromophore, whereas the Pt(II) units induce a significant red-shift. This signals that there is greater mixing of the metal orbitals with the π electron system in the ET-Cbz-TE chromophore for the Pt(II) systems. This results in greater metal induced spin-orbit coupling in the Pt(II) systems, and the effect is manifested in a reduced fluorescence yield and higher phosphorescence yield for CBZ-Poly-Pt \sim CBZ-Pt-1. All of the systems investigated exhibit moderately intense mid-visible transient absorption from a triplet state with a lifetime in the sub-microsecond timescale, consistent with relatively efficient intersystem crossing. Femtosecond non-linear transmittance experiments were utilized to construct the 2-photon absorption spectra of the chromophores. In each case, the 2PA absorption is blue shifted relative to the transition that is degenerate with the primary ground state absorption band. This result is consistent with the centrosymmetric structure of the metallated ET-Cbz-TE chromophore structure. The peak 2PA for this series occurs in the region 550–600 nm with σ_2 values >800 GM.

While the overall non-linear response of this series of organometallic oligomers to nanosecond pulses is lower than

that seen in previous studies of Pt-acetylide chromophores, the excellent visible transparency of the ET-Cbz-TE family makes this system promising for non-linear optical applications where transparency for $\lambda < 500$ nm is a requirement.

Acknowledgements

This work is supported by Air Force Office of Scientific Research (grant AFOSR FA-9550-06-1-1084) and National Science Foundation (grant no. CHE-115164). The work at Montana State University is supported by Air Force Office of Scientific Research (grant no. FA9550-09-1-0219) and Estonian Science Foundation (grant ETF no. 4977).

References

- 1 M. Göppert-Mayer, *Ann. Phys.*, 1931, **401**, 273–294.
- 2 W. Kaiser and C. G. B. Garrett, *Phys. Rev. Lett.*, 1961, **7**, 229–231.
- 3 R. Westlund, E. Malmström, C. Lopes, J. Öhgren, T. Rodgers, Y. Saito, S. Kawata, E. Glimsdal and M. Lindgren, *Adv. Funct. Mater.*, 2008, **18**, 1939–1948.
- 4 C. Tang, Q. Zheng, H. Zhu, L. Wang, S.-C. Chen, E. Ma and X. Chen, *J. Mater. Chem. C*, 2013, **1**, 1771–1780.
- 5 C. W. Spangler, *J. Mater. Chem.*, 1999, **9**, 2013–2020.
- 6 K. D. Belfield, M. V. Bondar, F. E. Hernandez and O. V. Przhonska, *J. Phys. Chem. C*, 2008, **112**, 5618–5622.
- 7 S. Kim, T. Y. Ohulchanskyy, H. E. Pudavar, R. K. Pandey and P. N. Prasad, *J. Am. Chem. Soc.*, 2007, **129**, 2669–2675.
- 8 W. Denk, J. Strickler and W. Webb, *Science*, 1990, **248**, 73–76.
- 9 D. A. Parthenopoulos and P. M. Rentzepis, *Science*, 1989, **245**, 843–845.
- 10 H. E. Pudavar, M. P. Joshi, P. N. Prasad and B. A. Reinhardt, *Appl. Phys. Lett.*, 1999, **74**, 1338–1340.
- 11 D. Day, M. Gu and A. Smallridge, *Opt. Lett.*, 1999, **24**, 948–950.
- 12 N. J. Long, *Angew. Chem., Int. Ed. Engl.*, 1995, **34**, 21–38.
- 13 J. E. Rogers, J. E. Slagle, D. M. Krein, A. R. Burke, B. C. Hall, A. Fratini, D. G. McLean, P. A. Fleitz, T. M. Cooper, M. Drobizhev, N. S. Makarov, A. Rebane, K.-Y. Kim, R. Farley and K. S. Schanze, *Inorg. Chem.*, 2007, **46**, 6483–6494.
- 14 J. E. Haley, D. M. Krein, J. L. Monahan, A. R. Burke, D. G. McLean, J. E. Slagle, A. Fratini and T. M. Cooper, *J. Phys. Chem. A*, 2010, **115**, 265–273.
- 15 K.-Y. Kim, A. H. Shelton, M. Drobizhev, N. Makarov, A. Rebane and K. S. Schanze, *J. Phys. Chem. A*, 2010, **114**, 7003–7013.
- 16 K. A. Nguyen, P. N. Day and R. Pachter, *J. Phys. Chem. A*, 2009, **113**, 13943–13952.
- 17 Z.-D. Yang, J.-K. Feng and A.-M. Ren, *Inorg. Chem.*, 2008, **47**, 10841–10850.

- 18 G. G. Dubinina, R. S. Price, K. A. Abboud, G. Wicks, P. Wnuk, Y. Stepanenko, M. Drobizhev, A. Rebane and K. S. Schanze, *J. Am. Chem. Soc.*, 2012, **134**, 19346–19349.
- 19 C. Liao, A. H. Shelton, K.-Y. Kim and K. S. Schanze, *ACS Appl. Mater. Interfaces*, 2011, **3**, 3225–3238.
- 20 K. McEwan, K. Lewis, G. Y. Yang, L. L. Chng, Y. W. Lee, W. P. Lau and K. S. Lai, *Adv. Funct. Mater.*, 2003, **13**, 863–867.
- 21 T. C. Wen and C. Y. Tsai, *Chem. Phys. Lett.*, 1999, **311**, 173–178.
- 22 J. L. Humphrey and D. Kuciauskas, *J. Am. Chem. Soc.*, 2006, **128**, 3902–3903.
- 23 T. E. O. Screen, J. R. G. Thorne, R. G. Denning, D. G. Bucknall and H. L. Anderson, *J. Mater. Chem.*, 2003, **13**, 2796–2808.
- 24 J. W. Perry, D. Alvarez, I. Choong, K. Mansour, S. R. Marder and K. J. Perry, *Opt. Lett.*, 1994, **19**, 625–627.
- 25 D. Swain, R. Singh, V. K. Singh, N. V. Krishna, L. Giribabu and S. V. Rao, *J. Mater. Chem. C*, 2014, **2**, 1711–1722.
- 26 B. S. Wang, J. Wang and J.-Y. Chen, *J. Mater. Chem. B*, 2014, **2**, 1594–1602.
- 27 R. Liu, H. Chen, J. Chang, Y. Li, H. Zhu and W. Sun, *Dalton Trans.*, 2013, **42**, 160–171.
- 28 S. M. Aly, C.-L. Ho, W.-Y. Wong, D. Fortin and P. D. Harvey, *Macromolecules*, 2009, **42**, 6902–6916.
- 29 C.-L. Ho, C.-H. Chui, W.-Y. Wong, S. M. Aly, D. Fortin, P. D. Harvey, B. Yao, Z. Xie and L. Wang, *Macromol. Chem. Phys.*, 2009, **210**, 1786–1798.
- 30 J. B. Seneclauze, P. Retailleau and R. Ziessel, *New J. Chem.*, 2007, **31**, 1412–1416.
- 31 N. Zhang, A. Hayer, M. K. Al-Suti, R. A. Al-Belushi, M. S. Khan and A. Köhler, *J. Chem. Phys.*, 2006, **124**, 244701.
- 32 G.-J. Zhou, W.-Y. Wong, D. Cui and C. Ye, *Chem. Mater.*, 2005, **17**, 5209–5217.
- 33 C.-H. Tao, H. Yang, N. Zhu, V. W.-W. Yam and S.-J. Xu, *Organometallics*, 2008, **27**, 5453–5458.
- 34 A. Tacca, R. Po, M. Caldararo, S. Chiaberge, L. Gila, L. Longo, P. R. Mussini, A. Pellegrino, N. Perin, M. Salvalaggio, A. Savoini and S. Spera, *Electrochim. Acta*, 2011, **56**, 6638–6653.
- 35 W. Lu, W.-M. Kwok, C. Ma, C. T.-L. Chan, M.-X. Zhu and C.-M. Che, *J. Am. Chem. Soc.*, 2011, **133**, 14120–14135.
- 36 C. Ma, C. T.-L. Chan, W.-M. Kwok and C.-M. Che, *Chem. Sci.*, 2012, **3**, 1883–1892.
- 37 G. S. M. Tong, P. K. Chow and C.-M. Che, *Angew. Chem., Int. Ed.*, 2010, **49**, 9206–9209.
- 38 N. S. Makarov, M. Drobizhev and A. Rebane, *Opt. Express*, 2008, **16**, 4029–4047.
- 39 A. Rebane, M. Drobizhev, N. S. Makarov, G. Wicks, P. Wnuk, Y. Stepanenko, J. E. Haley, D. M. Krein, J. L. Fore, A. R. Burke, J. Slagle, D. G. McLean and T. M. Cooper, *J. Phys. Chem. A*, 2014, **118**, 3749–3759.
- 40 M. Sheik-Bahae, A. A. Said, T.-H. Wei, D. J. Hagan and E. W. Van Stryland, *IEEE J. Quantum Electron.*, 1990, **26**, 760–769.
- 41 D. A. Oulianov, I. V. Tomov, P. M. Dvornikov and P. M. Rentzepis, *Opt. Commun.*, 2001, **191**, 235–243.
- 42 H.-Y. Chao, W. Lu, Y. Li, M. C. W. Chan, C.-M. Che, K.-K. Cheung and N. Zhu, *J. Am. Chem. Soc.*, 2002, **124**, 14696–14706.
- 43 W.-Y. Wong, L. Liu, S.-Y. Poon, K.-H. Choi, K.-W. Cheah and J.-X. Shi, *Macromolecules*, 2004, **37**, 4496–4504.
- 44 S.-i. Kato, S. Shimizu, H. Taguchi, A. Kobayashi, S. Tobita and Y. Nakamura, *J. Org. Chem.*, 2012, **77**, 3222–3232.
- 45 M. Montalti, A. Credi, L. Prodi and M. T. Gandolfi, in *Handbook of Photochemistry*, 3rd edn, 2005, ch. 13.
- 46 G.-J. Zhou and W.-Y. Wong, *Chem. Soc. Rev.*, 2011, **40**, 2541–2566.
- 47 A. Parthasarathy, S. Goswami, T. S. Corbitt, E. Ji, D. Dascier, D. G. Whitten and K. S. Schanze, *ACS Appl. Mater. Interfaces*, 2013, **5**, 4516–4520.
- 48 F. Terenziani, A. Painelli, C. Katan, M. Charlot and M. Blanchard-Desce, *J. Am. Chem. Soc.*, 2006, **128**, 15742–15755.
- 49 G. G. Dubinina, R. S. Price, K. A. Abboud, G. Wicks, P. Wnuk, Y. Stepanenko, M. Drobizhev, A. Rebane and K. S. Schanze, *J. Am. Chem. Soc.*, 2012, **134**, 19346–19349.